

# Nanoindentation of Thin Films Prepared by Physical Vapor Deposition

Dhiflaoui Hafedh, Khelifi Kaouthar, Ben Cheikh Larbi Ahmed

**Abstract**—These Monolayer and multilayer coatings of CrN and AlCrN deposited on 100Cr6 (AISI 52100) substrate by PVD magnetron sputtering system. The microstructures of the coatings were characterized using atomic force microscopy (AFM). The AFM analysis revealed the presence of domes and craters that are uniformly distributed over all surfaces of the various layers. Nanoindentation measurement of CrN coating showed maximum hardness (H) and modulus (E) of 14 GPa and 190 GPa, respectively. The measured H and E values of AlCrN coatings were found to be 30 GPa and 382 GPa, respectively. The improved hardness in both the coatings was attributed mainly to a reduction in crystallite size and decrease in surface roughness. The incorporation of Al into the CrN coatings has improved both hardness and Young's modulus.

**Keywords**—CrN/AlCrN, coatings, hardness, nano-indentation.

## I. INTRODUCTION

PHYSICAL VAPOR DEPOSITION (PVD) is a wide spread method for preparing thin coatings on tool steels. It is well known that transition metal nitride hard coatings prepared by plasma assisted Physical Vapor Deposition (PVD) techniques can be widely applied to improve the performance and lifetime of industrial tools and machine parts [1]-[3].

Amongst them, CrN coatings have been shown to have attractive properties, such as a high oxidation temperature and excellent corrosion resistance under severe environmental conditions [4].

To further improve the general performance of CrN coatings, alloying with another metal to form multicomponent coatings has been undertaken [5], [6].

The level of performance of such layers depends on their composition and structure, the deposition parameters and also the reliability of the technologies associated with measurement of characteristics commonly represented by the hardness and modulus of elasticity of thin films. The hardness to elastic ratio (H/E) provides regarding the relative importance of plastic (irreversible) and elastic (reversible) deformations [7].

The addition of aluminum effect in a binary CrN on coating adhesion has been studied in other works [3]. However, there are a few reports on the composition influence and the CrN/CrAlN structure's multilayer coatings on the mechanical behavior and the advantage of compared-structure multilayer to the single layer structure.

The aim of the presented investigation was to study available nitride coatings. Hardness has been obtained both in

the nano-indentation regimes, and the response of the coated systems has been analyzed in terms of their structure.

## II. EXPERIMENTS

All coatings were deposited on 100C6 steel (AISI 52100) in a commercial PVD magnetron sputter unit from Balzers (French). The targets were either pure chromium or aluminum. Nitrogen gas (99.995%) was used to deposit CrN or AlCrN. To improve the adhesion, a metallic Cr layer was deposited before the layer of CrN or AlCrN.

Aluminum/chromium material were placed as targets on the inner sides of the chamber walls to deposit AlCrN coating, onto the tool substrate, and a substrate current of 18.5 A was supplied. The argon and N<sub>2</sub> gases were supplied into the chamber, and the gas pressures were maintained on the basis of the chamber pressure.

## III. RESULTS AND DISCUSSION

### A. Coatings Composition

Glow Discharge Optical Emission Spectroscopy (GDOES) analysis is shown in Fig. 1.

The profile obtained with the coating of CrN (Fig. 1) shows the presence of 55% of Cr and 45% of N. It comprises, successively, a first buffer layer of chromium (100 nm), an intermediate layer of CrN (3 microns) and a layer of CrAlN (3.1 microns). The intermediate layer is made of CrN, on average 49% chromium, and 51% of nitrogen, while the layer of CrAlN consists of 25% chromium, 24% aluminum and 51% nitrogen. Under these conditions the crystal structure of CrAlN is fcc B1 type.

### B. Coatings Morphology

Using the AFM observations we determined the surface morphology. The surfaces were globally uniform and covered with domes and tiny craters (Fig. 2).

The scanner extends the tip along the Z axis to probe for the sample surface. The surface was scanned at a maximum speed of 0.1 mm/s to a range of 10 to 110  $\mu$ m. The AFM results for surface roughness values show that the CrN coating roughness values (14 nm) was smaller than those of the AlCrN coating (58 nm). The AlCrN coating exhibit surface irregularities and pits; these coatings have higher surface roughness values compared to that of the CrN coating.

### C. Residual Stress

Residual stresses values of CrN single layer and CrN/CrAlN multilayer coatings were determined by XRD using the  $\sin^2\psi$  method; the results are illustrated in Table I.

Dhiflaoui Hafedh, Khelifi Kaouthar, and Ben C. L. Ahmed are with Laboratoire Mécanique Matériaux et Procédés, Ecole Supérieure des Sciences et Techniques de Tunis, University of Tunis, Tunisia (e-mail: dhafedh@gmail.com).

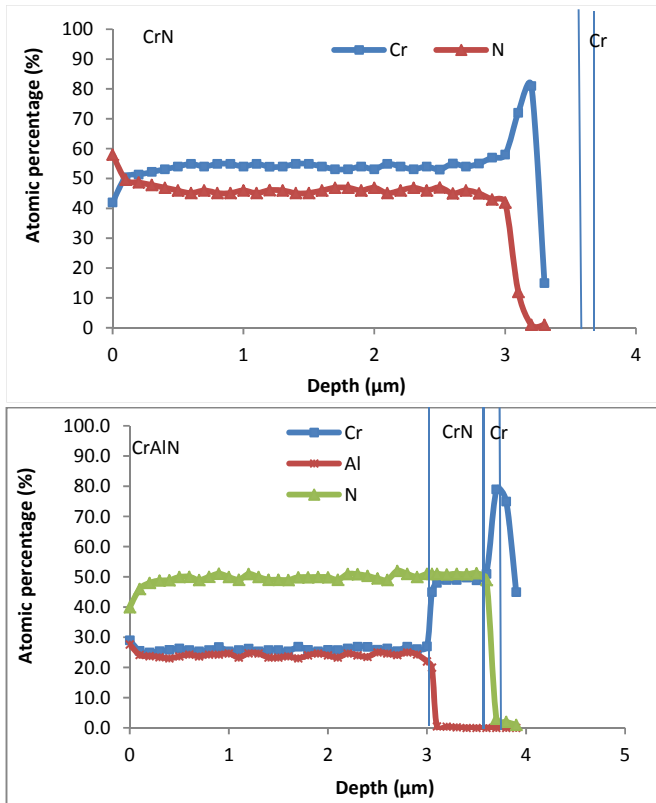


Fig. 1 The Profile of CrN and CrAlN coatings composition

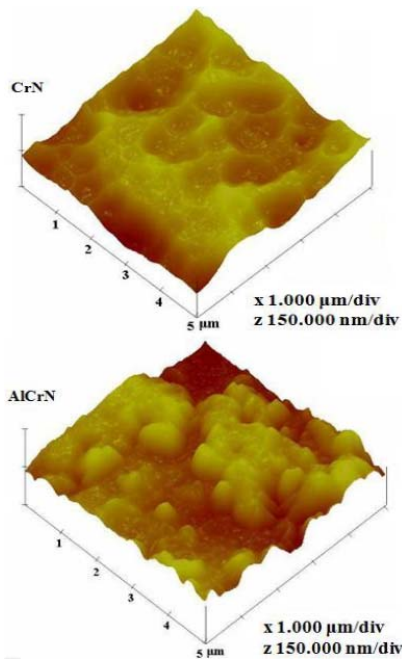


Fig. 2 Three-dimensional AFM images of CrN and AlCrN coatings

TABLE I  
THICKNESS, ROUGHNESS, AND RESIDUAL STRESSES OF CRN MONOLAYER AND CRALN MULTILAYER

Coatings	Thickness (μm)	Roughness (nm)	Residual stresses (GPa)
CrN monolayer	3.2	14	- 1.75
CrN/CrAlN multilayer	3.8	58	-3

It was indicated that the values of residual stresses vary from one coating to another. However, all coatings were characterized by compressive stresses type. Indeed, for the same thickness, residual compressive stresses increase when the coating consists of several layers. Multilayer structure offered the highest residual stresses values. This result has two origins. The first one is the thermo-mechanical stresses due to the difference in thermal expansion coefficient ( $11.7 \times 10^{-6} \text{K}^{-1}$  for the substrate,  $5.75 \times 10^{-6} \text{K}^{-1}$  for the CrN and  $8 \times 10^{-6} \text{K}^{-1}$  for the Cr) and the difference of Young's modulus in each interface such as between Cr and substrate, between CrN and Cr and between CrN and CrAlN (Fig. 3). The second origin is the intrinsic stresses due to the growth mechanisms of the coatings.

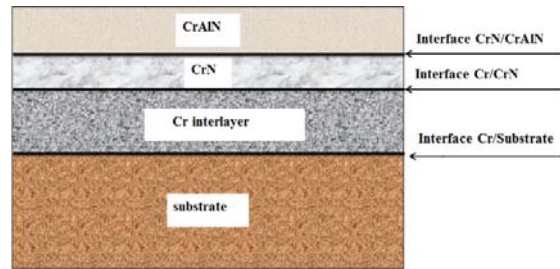


Fig. 3 Schematic illustration of CrN/CrAlN multilayer

#### D. Nanoindentation Tests

The nanoindentation tests were realized to measure the hardness and the Young's modulus of the coatings. A Berkovich diamond indenter was used to make indentations. The measurements of hardness and Young's modulus are mainly based on the unloading curve according to the Oliver and Pharr method [8].

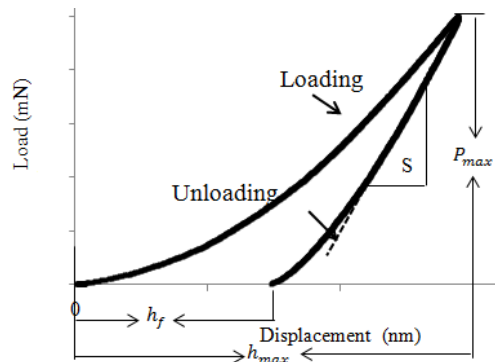


Fig. 4 Typical indentation loading-unloading curve

There are three important quantities that must be measured from P-h curves: the maximum load,  $P_{max}$ , the maximum displacement,  $h_{max}$ , and the elastic unloading stiffness,  $S = dP/dh$ , defined as the slope of the upper portion of the unloading curve during the initial stages of unloading (also called contact stiffness). Another important quantity is the final depth,  $h_f$ , the permanent depth of penetration after the indenter is fully unloaded. The hardness is estimated from:

$$H = P/A \quad (1)$$

Measurement of the elastic modulus follows from its relationship to contact area and the measured unloading stiffness through the relation:

$$S = \beta \frac{2}{\sqrt{\pi}} E_{eff} \sqrt{A_c} \quad (2)$$

where  $E_{eff}$  is the effective elastic modulus defined by:

$$\frac{1}{E_{eff}} = \frac{1-\nu^2}{E} + \frac{1-\nu_i^2}{E_i} \quad (3)$$

The effective modulus takes into account the fact that elastic displacements occur in both the specimen, with Young's modulus  $E$  and Poisson's ratio  $\nu$ , and the indenter, with elastic constants  $E_i$  and  $\nu_i$ . The loading/unloading curve show similar responses with respect to stiffness and deformation.

Fig. 5 shows the evolution of the hardness as a function of displacement. It was found that hardness exudes a maximum value in the smaller displacement. This requires reflection on the indentation limit that allows avoiding the effects of the substrate. It is also recommended that the nanoindentation test must be performed much less than 1/10th of the film thickness.

Figs. 6 and 7 show the variation of mechanical proprieties as a function of coatings structures. The hardness of the CrN monolayer was 14 GPa and the modulus was about 190 GPa. This must be related to the production conditions of the coating, especially the polarization voltage (-100 V). Further work showed that CrN can provide, with the same crystal structure and the same chemical composition as those obtained in the study, a hardness of the order of 23 GPa and a modulus 390 GPa. The failure of CrN encountered in this study is the column density of the layer growth. The addition of aluminum in the CrN and increasing the polarization voltage has been beneficial to the mechanical properties because the hardness is increased to 30 GPa and modulus to 382 GPa. The substitution of aluminum chromium produces a decrease in crystal lattice parameters; this reduction has a significant effect on the mechanical properties of CrN/CrAlN. The second hardening source is linked to the polarization voltage, increasing compared to that of CrN, provides a more marked columns growth density of the coating.

#### IV. CONCLUSIONS

CrN and AlCrN coatings were deposited on AISI 52100 substrates with the PVD technique using radio frequency magnetron sputtering. The morphological was evaluated using an atomic force microscopy (AFM). Hardness and Young's modulus as fundamentals mechanical properties were evaluated with nanoindentation test. It was found that the CrN coating has low roughness (14 nm), the AlCrN coating have greater surface roughness value of 58 nm. The nanoindentation test results show that the AlCrN coating has a hardness of 30 GPa and a Young's modulus of 382 GPa. The CrN coating has a lower hardness of 14 GPa and a Young's modulus of 190 GPa.

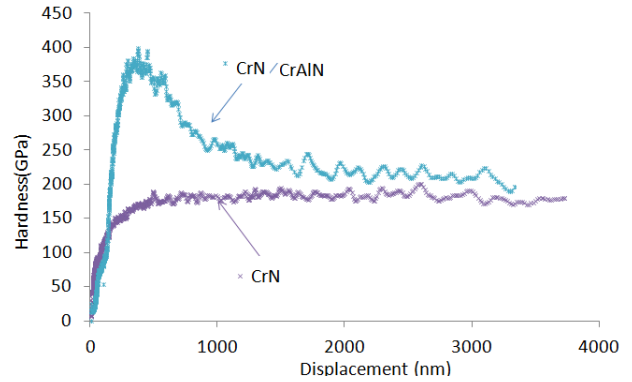


Fig. 5 Hardness vs. displacement curve for CrN and CrAlN coatings

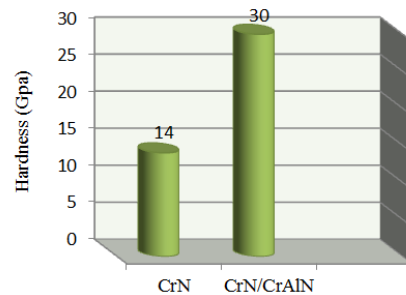


Fig. 6 Hardness vs. coatings structure (CrN monolayer and CrN/CrAlN multilayer)

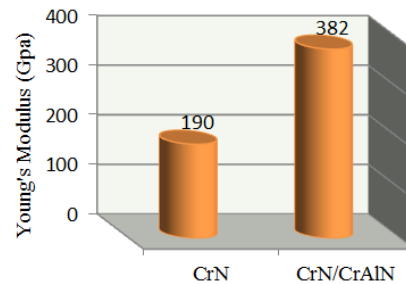


Fig. 7 Modulus vs. coatings structure (CrN monolayer and CrAlN multilayer)

TABLE II  
MECHANICAL PROPERTIES OF COATINGS CALCULATED FROM THE NANO INDENTATION TEST

Coatings	Thickness ( $\mu\text{m}$ )	H/E	H <sup>3</sup> /E*2 (GPa)
CrN monolayer	3.2	0.058	0.048
CrN/CrAlN multilayer	3.8	0.079	0.185

The coatings resistance to elastic-plastic deformation is controlled by their hardness and modulus. Results are illustrated in Table II. The resistance to elastic deformation is related to the ratio of the hardness and the modulus  $H/E$ , and the resistance to plastic deformation is related to  $H^3/E^2$  [9], [10]. A higher value of  $H^3/E^2$  and  $H/E$  that characterizes the CrN/CrAlN multilayer coating. This indicated a high resistance to elastic-plastic deformation of this coating. This result is expected from a coating with the highest hardness, modulus, compressive stresses and number of interfaces.

#### ACKNOWLEDGMENT

Authors acknowledge the help of LMMP (Laboratory of Mechanics, Materials, and Processes) of ENSIT, University of Tunis and Balzers Group.

#### REFERENCES

- [1] K. Holmberg, A. Matthews, "Tribology: Properties, mechanisms, techniques and applications in surface engineering," in *Coating tribology* vol. 56, 2009.
- [2] M. Van Stappen, K. M. Stales, M. Kerkhofs, C. Quacyhaegens "State of the art for the industrial use of ceramic PVD coatings," in *Surf. Coat. Technol* vol. 629, 2013, pp. 85-96.
- [3] K. Khelifi, A. Ben Cheikh Larbi "Mechanical properties and adhesion of TiN monolayer and TiN/TiAlN nanolayer coatings," in *Journal of Adhesion Science and Technology*, 1995, pp. 74-75.
- [4] B. Navinsek, P. Panjan, I. Milosev "Industrial applications of CrN (PVD) coatings, deposited at high and low temperatures," in *Surf. Coat. Technol*, 1997, pp 182.
- [5] H. A. Jehn, "Multicomponent and multiphase hard coatings for tribological applications," in *Surf. Coat. Technol*, 2000, pp 433-440.
- [6] H. Hasegawa, T. Suzuki "Effects of second metal contents on microstructure method" *Surf. Coat. Technol*, 2004, pp 188-189.
- [7] M. Kawate, A. K. Hashimoto, T. Suzuki "Oxidation resistance of CrAlN and TiAlN films," in *Surf. Coat. Technol*, 2003, pp 163-167.
- [8] A. C. Fischer-Cripps, "Critical review of analysis and interpretation of nanoindentation test," in *Surf. Coat. Technol*, 2006, pp 4153.
- [9] Lv F, Wen SP, Zong RL, Zeng F, Gao Y, Pan F. "Nanoindentation study of amorphous-Co79Zr13Nb8/Cr multilayers," in *Surf. Coat. Technol*. 2008, 202, pp3239–3245.
- [10] Harish C. Barshilia , N. Selvakumar, B. Deepthi, K.S. Rajam, "A comparative study of reactive direct current magnetron sputtered CrAlN and CrN coatings," in *Surface & Coatings Technology* ., 2006, 201, pp2193–2201.